applied sciences

MDPI

Article

Poly(phenylene methylene)-Based Coatings for Corrosion Protection: Replacement of Additives by Use of Copolymers

Marco F. D'Elia [1,*], Mirko Magni [2], Stefano P. M. Trasatti [2,*], Thomas B. Schweizer [1], Markus Niederberger [1] and Walter Caseri [1]

[1] Department of Materials, ETH Zürich, 8093 Zürich, Switzerland
[2] Department of Environmental Science and Policy, University of Milan, 20133 Milan, Italy
* Correspondence: marco.delia@mat.ethz.ch (M.F.D.); stefano.trasatti@unimi.it (S.P.M.T.)

Received: 17 July 2019; Accepted: 27 August 2019; Published: 29 August 2019

Abstract: Poly(phenylene methylene) (PPM) is a thermally stable, hydrophobic, fluorescent hydrocarbon polymer. Recently, blended PPM has been proposed as a valuable anti-corrosion coating material, and, in particular, rheological additives such as external plasticizers resulted crucial to prevent crack formation. Accordingly, to avoid common problems related to the use of external plasticizers, the development of PPM-related copolymer-based coatings containing *n*-octyloxy side chains and their anti-corrosion behavior were explored in this study. The aluminum alloy AA2024, widely employed for corrosion studies, was selected as a substrate, covered with a thin layer of a polybenzylsiloxane in order to improve adhesion between the underlying hydrophilic substrate and the top hydrophobic coating. Gratifyingly, coatings with those copolymers were free of bubbles and cracks. The *n*-octyloxy side-chains may be regarded to adopt the role of a bound plasticizer, as the glass transition temperature of the copolymers decreases with increasing content of alkoxy side-chains. Electrochemical corrosion tests on PPM-substituted coatings exhibited good corrosion protection of the metal surface towards a naturally aerated near-neutrally 3.5% wt.% NaCl neutral solution, providing comparable results to blended PPM formulations, previously reported. Hence, the application of rheological additives can be avoided by use of proper design copolymers.

Keywords: poly(phenylene methylene) coatings; PPM-related copolymer; rheological additive-free polymer formulation; AA2024; corrosion protection; electrochemistry

1. Introduction

Poly(phenylene methylene) (PPM) is a hydrocarbon polymer with the general formula $(C_6H_4[CH_2])_n$. It is structurally located between polyethylene and polyphenylene, consisting of an alternating sequence of phenylene and methylene units (Figure 1a). Remarkably, it exhibits a rather unique combination of material properties. Besides high hydrophobicity [1], it is highly thermally stable (onset of decomposition temperature at 450–470 °C) [2–5] and fluorescent [6]. This optical property, unusual for a non-conjugated polymer such as PPM, was attributed to homoconjugation [6]. The rare phenomenon of homoconjugation can arise under particular geometric conditions when conjugated π-orbital systems interact with each other, even though they are electronically separated by an insulating methylene group [7,8], as illustrated in Figure 1b.

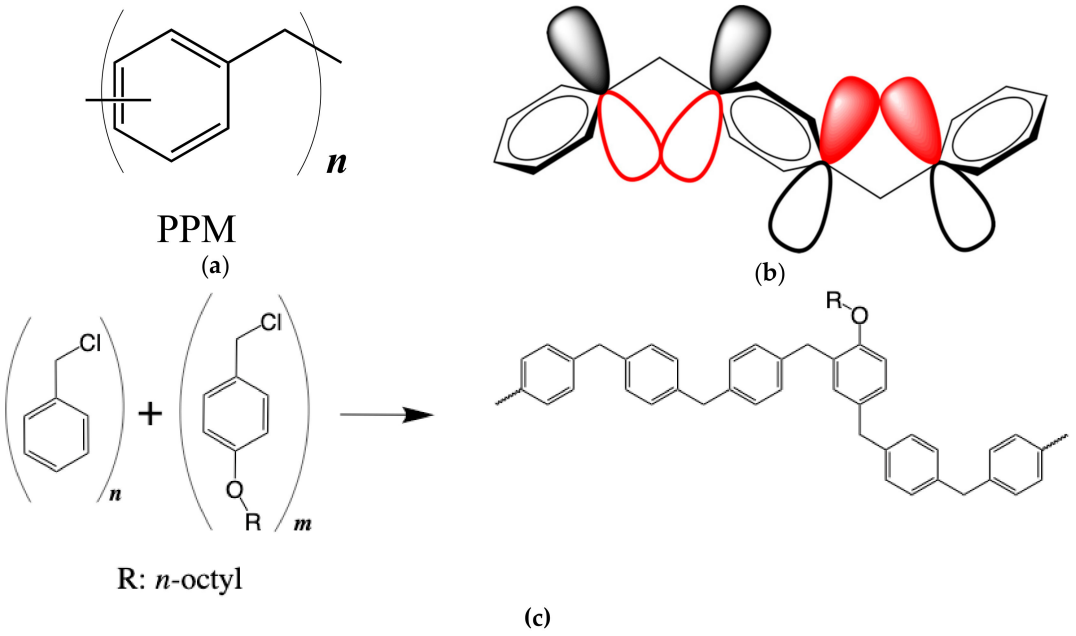

Figure 1. (**a**) Repeating units of poly(phenylene methylene) (PPM), (**b**) schematic representation of homoconjugation in PPM: p-orbitals of phenylene rings overlap even if they are electronically separated by methylene group, (**c**) scheme of the synthesis of random copolymers based on PPM obtained by mixing different fractions (*n* and *m*, *m*/(*m*+*n*) = 5.3% mol/mol or 11.2% mol/mol) of benzyl chloride and its derivative (4-octyloxybenzyl chloride), and structure of a sequence of the resulting random copolymers.

Moreover, importantly, PPM has also been shown to be effective in corrosion protection, however, only when blended with rheological additives, such as polysiloxanes and benzylbutyl phthalate, as an external plasticizer in order to prevent cracking of the surface due to the stiffness of the polymer [1]. Notably, the principal aim of plasticizers is to ameliorate the elasticity and processability of polymers by lowering the second order transition temperature (glass transition temperature), thus decreasing the tendency of coatings to formation of cracks [1,9]. More specifically, external plasticizers are low molar mass compounds which are dispersed in the polymeric matrix spreading the polymer chains apart [10]. Thus, plasticizers depress the polymer–polymer secondary interactions into the polymeric matrix enhancing the mobility of the polymer chains, resulting in a softer material which can be easily deformed. However, due to the weak interactions between polymer chains and external plasticizers, the plasticizer can leave the material matrix by evaporation, migration or extraction, and upon exposure to UV light the plasticizer can degrade and subsequently also initiate degradation of the polymer [11,12]. Further, external plasticizers can increase the erodibility of the coating, thus reducing the material's lifetime [10,12].

However, migration of external plasticizers and the film-forming properties of polymers can be managed by application of polymer-bound molecules which can quasi be regarded as internal plasticizers [13]. In particular, the presence of bulky side chains along the polymer backbone lowers the internal forces between the polymer main chains [13,14].

In this way, we sought to design a copolymer based on phenylene methylene units for corrosion protection, by inserting different fractions of *n*-octyloxy side chains into the PPM backbone. The poly(phenylene methylene) derivative was synthesized by copolymerization of a mixture of benzyl chloride and variable fractions of 4-octylbenzyl chloride in presence of tin tetrachloride as catalyst, analogously to the synthesis of PPM itself [2].

Hence, in this presented work, the preparation of corrosion-resistant PPM-related coatings on pretreated aluminum alloy AA2024 containing different molar fractions of *n*-octyloxy side chains (Figure 1c) were prepared to explore the efficacy of long alkoxy side-chains as a reliable

alternative to rheological additives. Accordingly, the ability of PPM derivatives in anti-corrosion protection was examined by coating pretreated aluminum alloy samples (AA2024) and studying their behavior in a naturally aerated near-neutral 0.6 M sodium chloride solution anodic polarization and potentiostatic polarization techniques. Additionally, thermal stability and glass transition temperature of the copolymers were investigated by thermogravimetric analysis (TGA) and differential scanning calorimetry (DSC).

2. Materials and Methods

2.1. Reagents and Solvents

Benzyl chloride stabilized by propylene oxide (99%), tin(IV) chloride, phosphoric acid (85%), thionyl chloride (99%), sodium sulfate (99%) and chloroform were purchased from Sigma Aldrich (Buchs, Switzerland), benzyltriethoxysilane from Fluorochem (Hadfield, UK), 4-hydroxybenzaldehyde (98%) and 1-bromooctane (98%) from abcr (Karlsruhe, Germany), sodium borohydride (98%) and tetrahydrofuran (CROMANORM) from VWR Chemicals BDH (Leuven, Belgium), acetonitrile (99.9%), dichloromethane (99.8%), sodium hydroxide (98.66%) and potassium hydroxide (86%) from Fischer Chemicals (Loughborough, UK), and methanol (98%) from Merck (Darmstadt, Germany).

2.2. Apparatus

^{1}H NMR spectra were recorded on a Bruker AV 300 MHz (Billerica, MA, USA) instrument using $CDCl_3$ as solvent. Chemical shifts (δ) for 1H spectra are expressed in ppm relative to internal Me_4Si as standard. Signals were abbreviated as s, singlet; d, doublet; t, triplet; m, multiplet.

Elemental analysis was performed by the Microanalytic Laboratory of Organic Chemistry (LOC) at ETH Zürich.

Gel permeation chromatography (GPC) analysis were performed by using Viscotek GPC system (Malvern, Worcs, UK) equipped with a pump and degasser (GPCmax VE2001, 1.0 mL min^{-1} flow rate), a detector module (Viscotek 302 TDA) and three columns (2× PLGel Mix-C and 1× ViscoGEL GMHHRN 18055, dimensions 7.5 × 300 mm for each column) using tetrahydrofuran as an eluent.

Rheology measurements were carried out using an Anton-Paar MCR-302 rheometer with parallel plates (Graz, Austria), at a temperature of 120 °C. Complex viscosity was measured collecting 10 points at angular frequencies starting from 0.23–22 rad s^{-1} applying 5% of strain.

For thermogravimetric analysis (TGA), a Mettler Toledo TGA/DSC 3+ STAR^e system instrument (Mettler-Toledo, Schwerzenbach, Switzerland) was used heating the samples from 25 to 1000 °C with a heating rate of 10 °C min^{-1} under nitrogen atmosphere.

Differential scanning calorimetry (DSC) was carried out with a Mettler Toledo DSC822^e instrument (Columbus, OH, USA) using a cooling and heating rate of 10 °C min^1 under nitrogen atmosphere.

Pictures of polymer-coated AA2024 samples were obtained with an optical microscope (Wild Photomakroskop M400, Switzerland) equipped with a digital camera, combined with a portable UV lamp emitting at 395 nm (4 W, Lighting EVER).

Scanning Electron Microscopy (SEM)was performed with a LEO Gemini 1530.

2.3. Synthesis of 4-Octyloxybenzyl Chloride

4-Octyloxybenzyl chloride was synthesized according to the literature [15,16] as follows: 4-hydroxybenzaldehyde (0.16 mol, 20 g) was dissolved together with potassium hydroxide (0.2 mol, 11.12 g) in acetonitrile (270 mL) in a three-necked flask. The reaction was stirred at room temperature and heated to reflux at 90 °C. 1-Bromooctane (0.15 mol, 27 mL) was then added during 1 h and the reaction mixture was vigorously stirred overnight. Thereafter, the mixture was cooled to room temperature and quenched with 250 mL of water, transferred to a separatory funnel and extracted with hexane (200 mL). The organic layer was washed twice with 30 mL of NaOH solution (10% in mass) and finally with water (three times 30 mL). The organic phase was dried over anhydrous sodium

sulfate and concentrated in a rotary vapor at 300 mbar (40 °C) giving 4-octyloxy benzaldehyde as a pale-yellow oil (25.1 g, 0.11 mol, yield: 70%). ^{1}H NMR ($CDCl_3$): δ = 0.88 (t, 3H, CH_3), 1.19–1.55 (m, 10 H, 5 CH_2), 1.74–1.84 (m, 2H, CH_2), 4.01 (t, 2H, CH_2O), 6.65–6.98 (d, 2H, Ar), 7.79–7.82 (d, 2H, Ar), 9.85 (s, 1H, COH) ppm.

Afterwards, 4-octyloxy benzaldehyde (25.1 g, 0.107 mol) was dissolved in tetrahydrofuran (THF) (20 mL) and added dropwise to a stirred suspension of $NaBH_4$ (8.1 g, 0.2 mol) in dry THF (140 mL) at 0 °C. The reaction mixture was then warmed up to room temperature and stirred overnight. The reaction mixture was quenched with 50 mL of water and the organic layer was separated, washed with water (three times) and dried over anhydrous sodium sulfate [17]. The solvent was then removed by evaporation at 11 mbar and 40 °C, giving a white solid that was dissolved in 5 mL of THF and poured into 400 mL of water under stirring. The white precipitate was filtered (cellulose filter) and the cake was dried under vacuum (0.7 mbar) to give 4-octyloxybenzyl alcohol as a white powder (0.08 mol, 20.14 g, yield: 80%). ^{1}H NMR ($CDCl_3$): δ = 0.86–0.91 (t, 3H, CH_3), 1.20–1.49 (m, 10 H, 5 CH_2), 1.73–1.82 (m, 2H, CH_2), 3.93–3.95 (t, 2H, CH_2OAr), 4.61 (s, 2H, CH_2OH) 6.87–6.90 (d, 2H, Ar), 7.26–7.29 (d, 2H, Ar) ppm. $C_{15}H_{24}O_2$ (236.35 g mol^{-1}): calcd. C 76.23, H 10.23, found C 76.18, H 10.12.

Subsequently, 4-octcyloxybenzyl alcohol (0.03 mol, 7.08 g) was dissolved in dichloromethane (200 mL) and thionyl chloride (0.036 mol, 4.26 g) was added to the solution dropwise at 0 °C. The mixture was then stirred at the same temperature during 2 h and the reaction was subsequently quenched with water (100 mL). The organic layer was extracted, washed with water (40 mL) and saturated aqueous sodium hydrogen carbonate (140 mL) and dried over anhydrous sodium sulfate. The dichloromethane was evaporated at reduced pressure (100 mbar at 40 °C) obtaining 4-octyloxybenzyl chloride as a yellow pale oil (0.016 mol, 4.16 g, yield: 54%). ^{1}H NMR ($CDCl_3$): δ = 0.89–0.93 (t, 3H, CH_3), 1.31–1.49 (m, 10 H, 5 CH_2), 1.75–1.84 (m, 2H, CH_2), 3.94–3.98 (t, 2H, CH_2OAr), 4.57 (s, 2H, CH_2Cl) 6.87–6.90 (d, 2H, Ar), 7.29–7.32 (d, 2H, Ar) ppm. $C_{15}H_{24}OCl$ (254.80 g): calcd. C 70.71, H 9.10, found C 70.92, H 9.22.

2.4. Synthesis of the Octyloxy-Containing PPM Derivatives

Copolymerization of benzyl chloride in presence of 4-octyloxybenzyl chloride was performed with two ratios of the comonomers, 5.3% mol/mol and 11.2% mol/mol of 4-octyloxybenzyl chloride, respectively. First, propylene oxide stabilizer (0.25% w/v) was removed exposing benzyl chloride to vacuum (0.7 mbar) overnight. The removal of propylene oxide stabilizer was verified by ^{1}H NMR spectroscopy by disappearance of signals of propylene oxide at 2.96, 2.73, 2.41, and 1.31 ppm. In the case of 5.3% mol/mol, 1.58 g (1.6 mL, 6.2 mmol) of 4-octyloxybenzyl chloride was added under nitrogen atmosphere to 14.9 g (13.7 mL, 118 mmol) of destabilized benzyl chloride in a 100 mL three-neck flask equipped with a mechanical stirrer. In the case of 11.2% mol/mol, 1.49 g (1.50 mL 5.84 mmol) of 4-octyloxybenzyl chloride were added under nitrogen atmosphere to 6.1 mL (52 mmol) of destabilized benzyl chloride in a 100 mL three-neck flask equipped with a mechanical stirrer. Thereafter, the respective mixtures were heated up to 60 °C and 0.05 mL (0.46 mmol) of $SnCl_4$ was added. The copolymerizations were carried out under nitrogen flow of 0.4–0.5 mL min^{-1} to allow the produced HCl to leave the reaction environment. After 3 h, due to the increase of viscosity, the temperature was risen to 120 °C for 3 h and subsequently to 180 °C for 17 h. During the reaction, the color shifted from deep red after the addition of $SnCl_4$ to clear amber at the end of the reaction. Afterwards, the mixture was cooled down to room temperature and the product was solubilized in 10 mL of THF. This solution was then poured into 400 mL of methanol under vigorous stirring, and after 4 h, the obtained powder was filtered through a cellulose filter and dried under vacuum (10^{-2} mbar) for 12 h, yielding 3.87 g and 13.26 g of product, respectively, containing 13.4% and 6.1% of the octyloxy repeat units, respectively, as obtained from ^{1}H NMR spectra (see below). Accordingly, yields of 63% and 75%, respectively, were calculated in the case of 13.4% and 6.1% octyloxy repeat unit.

2.5. Preparation of Coated AA2024

Sheets of 12 cm in length, 3 cm in width and 4 mm in thickness of high strength aluminum alloy AA2024 (4.3%–4.5% copper, 1.3%–1.5% magnesium, 0.5%–0.6% manganese and less than 0.5% of other elements) were provided by Aviometal s.p.a (Varese, Italy) and used as substrate.

Samples of 4 cm in length were cut and subsequently polished with abrasive papers of 300, 500, 800, 1200, and 4000 grit. Immediately after polishing, the samples were cleaned by immersion in ethanol in an ultrasonic bath (Banderlin, Berlin, Germany) for 5 min. Then AA2024 samples were removed from the ethanol bath and the residual alcohol at the surface was evaporated by means of a flush of nitrogen.

A layer of benzyltriethoxysilane was applied by spin coating (3500 rpm, 30 s) on freshly cleaned AA2024 samples and subsequently heated up to 100 °C for 1 min, whereupon condensation of benzyltriethoxysilane to respective polysiloxanes proceeded [1]. These samples were finally coated with substituted PPM as described in the section Results and Discussion, using about 100 mg of polymer.

2.6. Electrochemical Characterization of Coated AA2024

The anticorrosion ability of the PPM derivatives as thin protective films was studied by means of electrochemistry techniques, carrying out tests on AA2024 samples coated with the two copolymers (6.1% mol/mol and 13.4% mol/mol). The protocol for the coating deposition is described in the Results and Discussion section.

Electrochemical corrosion tests were conducted in a naturally aerated near-neutral simulated marine environment prepared by dissolving 0.6 mol L^{-1} sodium chloride (≥99.0%, Sigma-Aldrich) in MilliQ® water. The pH value was adjusted to 6.7 ± 0.1 by adding few drops of 0.2 mol L^{-1} sodium hydroxide solution to the stock solutions. All the experiments, if not otherwise stated, were carried out at ambient temperature (24 ± 3 °C, with a variation lower than 2 °C during each single run). In all cases, the operative temperature was below the glass transition temperature of PPM derivatives (see below).

The apparatus used for the measurements consisted of a glass cell with a hole (1 cm in diameter) in the middle of the flat bottom part which assures the contact between the coated metallic plate (working electrode, exposed area 0.78 cm^2) and the working solution (0.6 M NaCl). The sealing was guaranteed by a bi-adhesive layer (a2 Soluzioni Adesive, Italy) pressed between the sample and the bottom of the cell. The electrochemical setup also included a platinum coil as counter electrode and an aqueous saturated calomel electrode as reference one (E_{SCE} = 0.242 V vs. SHE). The latter was inserted into a glass double bridge (filled with the same working solution) ending with a Luggin capillary aimed to minimize the ohmic drop between working and reference electrode. No instrumental compensation of the residual ohmic drop was performed.

The electrochemical characterization included both potentiodynamic and potentiostatic methods. The former consisted of a single anodic polarization scan, sweeping the potential from OCP to 2.5 V vs. SCE, at a scan rate of 10 mV min^{-1} (each run lasting ca. 5.5 h). A limit current density of 4 mA cm^{-2} was imposed, thereafter the scan was automatically aborted independently by the achievement of the final potential. The second characterization implies the application of a constant potential to the metallic sample and the recording of the current flow between working and counter electrode. In our experiments, an oxidizing potential of 0 V vs. SCE was applied for 24 h. Potentiodynamic and potentiostatic curves were recorded after an initial delay time of 600 s for assuring the equilibration of the system at OCP.

Some potentiodynamic curves were recorded also at a fixed temperature of 35 °C, just above the glass transition temperature of the modified PPM (see Results and Discussion). For these experiments, a suitable cell surrounded by a jacket filled by a flux of water controlled by a thermostat (Haake CH Fisons coupled to a Haake F3 Fision) was adopted.

3. Results and Discussion

3.1. Synthesis and Structural Characterization

PPM-based copolymers containing *n*-octyloxy side chains were obtained by mixing the comonomers benzyl chloride and 4-octyloxybenzyl chloride at two ratios, 5.3% mol/mol and 11.2% mol/mol, respectively, and polymerization was subsequently carried out under the conditions reported in the Materials and Methods section. For both ratios the number-average molar masses of the resulting copolymers (M_n) amounted to about 2500 g mol^{-1} and the weight-average molar masses (M_w) to about 5400 g mol^{-1}, resulting in polydispersity indices (PDI= M_w/M_n) of about 2.2–2.3 (Table 1). Notably, the fluorescence observed for PPM itself also emerged in the copolymers (Figure 2).

Table 1. Molar masses of copolymers prepared from benzyl chloride and 4-octylbenzyl chloride (6.1% mol/mol and 13.4% mol/mol).

Sample	Mn (g mol^{-1})	Mw (g mol^{-1})	PDI (Mw/Mn)
6.1% octyloxy units	2438	5402	2.21
13.4% octyloxy units	2382	5496	2.3

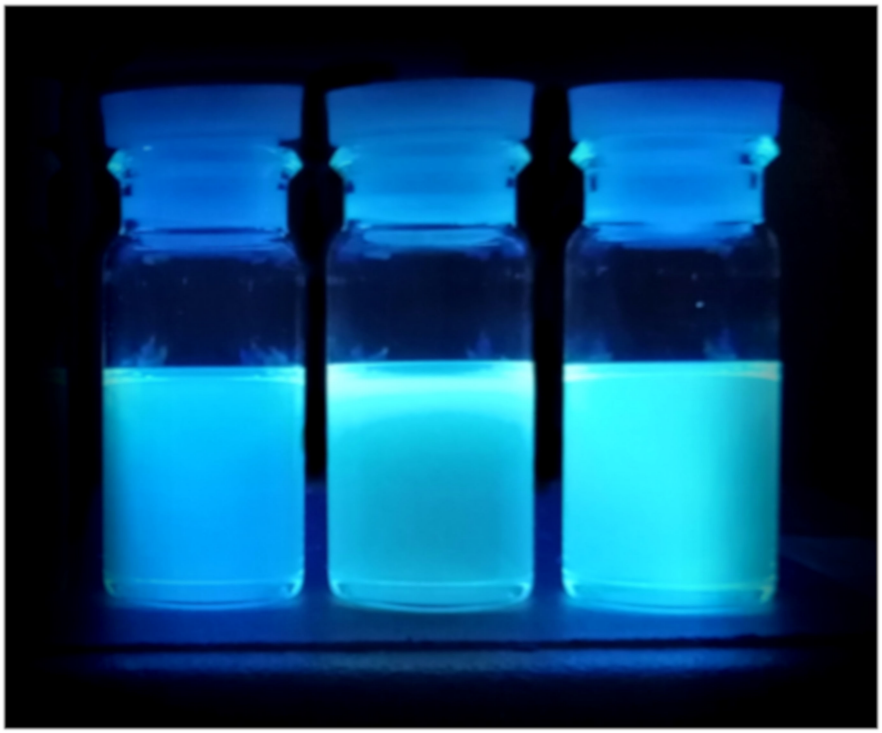

Figure 2. Photographs taken under UV-light illumination of PPM and its derivatives solutions in chloroform (≈0.5% m/m, 2 cm diameter of the vials): PPM (left), copolymer containing 13.4% (center) and 6.1% (right).

The presence of octyloxy groups in the copolymers was assessed with ^{1}H NMR spectroscopy. With regard to the reported values of PPM [18,19], ^{1}H NMR spectra of the copolymers showed the aromatic resonances (H_{Ar}) in the typical region of 6.8–7.2 ppm. The position of the bridging methylene signals (H_m) at 3.9 ppm differed from that of the corresponding signals of the CH_2Cl group of the comonomers at 4.5 ppm (Figure 3). Notably, the presence of the signals corresponding to the alkoxy chains (H_{Alk}) in the region of 0.5–1.5 ppm confirms the inclusion of octyloxy side chains into the polymers. Furthermore, the ratio between integrated peak areas of alkyl signals (H_{Alk}) and those of the methylene bridges (H_m) were used to calculate the effective molar composition of the copolymers. The obtained values

showed somewhat higher molar ratios of constitutional repeat units of the octyloxy groups (13.4% and 6.1%) than the comonomer ratio employed for the reaction (11.2% and 5.3% respectively). Obviously, polymers with a higher fraction of unsubstituted phenylene methylene units were removed during sample workup with somewhat higher preference.

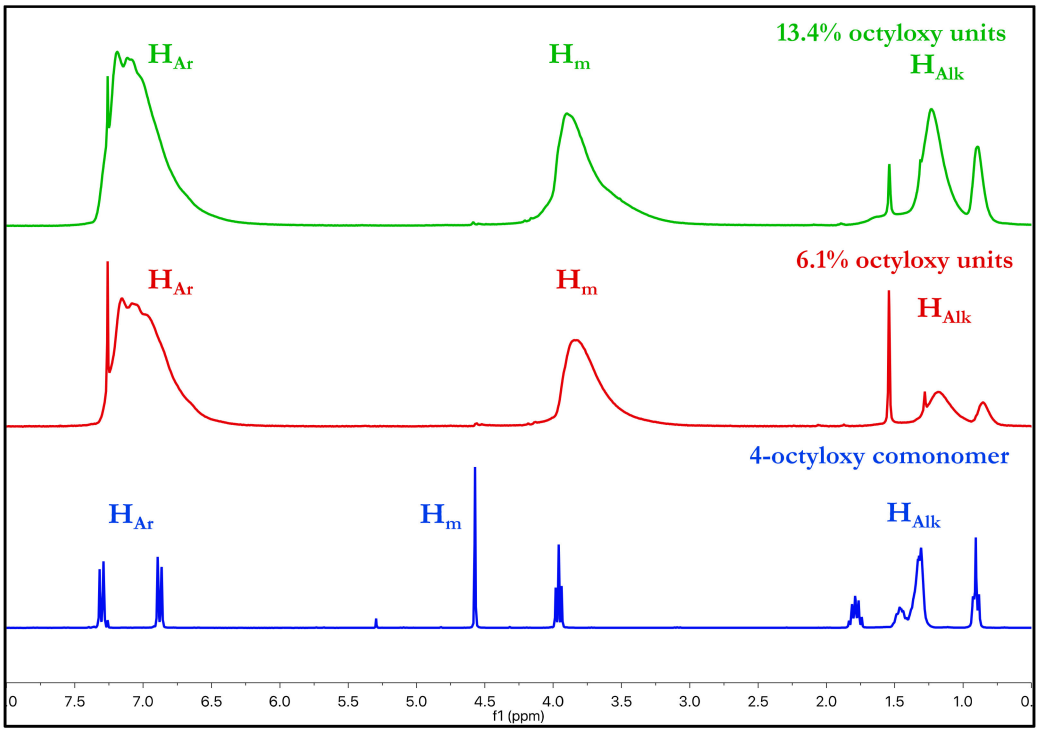

Figure 3. ^{1}H NMR spectra. From the bottom to top: 4-octyloxybenzyl chloride (blue line), copolymer with 6.1% mol/mol (red line), and 13.4% mol/mol 4-octyloxybenzyl-containing constitutional repeat units (green line).

3.2. Thermal Analysis

Thermogravimetric analysis of the polymers carried out under ambient atmosphere revealed an onset of thermal decomposition at about 380 and 400 °C respectively for PPM containing 13.4% mol/mol and 6.1% mol/mol of repeat units with alkoxy side chains, respectively, while the maximum decomposition rates were observed at 482 °C (for 13.4%) and 508 °C for (for 6.1%), compared to 510–515 °C for PPM itself [5,18].

Differential scanning calorimetry (DSC) performed with the copolymers revealed in each case only a single glass transition temperature (Table 2). The glass transition temperature (T_g) of the copolymers decreases as the fraction of the octyloxy side chains along the polymeric backbone increases. The pure PPM of M_n = 2400 g mol^{-1} features $T_g \approx$ 55 °C [2] while the PPM derivative containing 6.1% and 13.4% mol/mol of octyloxy side-chains exhibited T_g values of 48 and 31 °C, respectively (Table 2). This is likely due to the relative difference in mobility of the polymer chains, whose motion is progressively enhanced with the increase of the concentration of octyloxy substituents, leading to the corresponding decrease of T_g [20]. Moreover, the lack of any thermal transition beyond the glass transition temperature indicates that the copolymers are amorphous like PPM itself [6].

Table 2. Glass transition temperatures (T_g) and the difference between the temperature T applied in rheology experiments (120 °C and T_g), of PPM and copoylmers with (6.1% and 13.4% octyloxy groups, respectively.

Sample	T_g (°C)	(T-T_g) (°C)
PPM	55	65
6.1% octyloxy units	48	71
13.4% octyloxy units	31	89

3.3. Rheology

Dynamic rheological data of molten PPM and the related copolymers were obtained from frequency sweeps over the range of 0.3–22 rad s^{-1} at 5% strain at the temperature of 120 °C (the temperature of coating application). The applied 5% strain was confirmed to be within the linear viscoelastic region by strain sweep measurements. The complex viscosity (η*) of PPM and the copolymers are shown in Figure 4. The copolymer containing 6.1% mol/mol of *n*-octyloxy repeat units revealed a slight decrease of viscosity compared to PPM itself, while increasing the fraction of units with *n*-octyloxy side-chains to 13.4% mol/mol led a pronounced drop of viscosity (decrease by order of magnitude). It has to be noted that the measurements were performed at the film processing temperature (see below) which is well above the glass transition temperature of the polymers (Table 1). It appears, therefore, in agreement with glass transition temperatures, that *n*-octyloxy side-chains act as spacers between the polymer backbones decreasing the cumulative intermolecular forces along the polymer chains, thus inducing a decrease in viscosity.

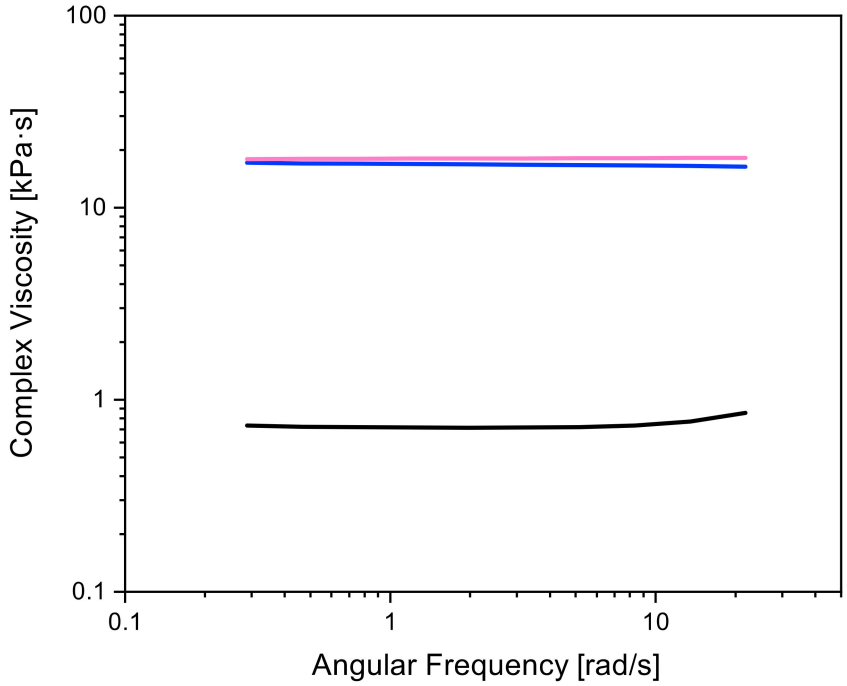

Figure 4. Effect of *n*-octyloxy side chains on the complex viscosity. From top to bottom: PPM (pink line), 6.1% mol/mol octyloxy units (blue line) and 13.4% mol/mol octyloxy units (black line).

3.4. Coatings

Coatings of the copolymers were manufactured by pressing polymer powders onto a silane-pretreated [1] AA2024 specimen, using polyetheretherketone (PEEK) foil to separate the PPM-based polymers from the pressing instrument. Pressing was performed for both copolymers (6.1% mol/mol and 13.4% mol/mol octyloxy units) at a temperature of 120 °C for 30 s. The thickness

of the resulting films was about 30 µm (Figures S1 and S2), and the coatings appeared very uniform and homogeneous although no rheological additive was added (Figure 5). Notably, at the processing temperature, the low viscosity of the molten polymer with 13.4% mol/mol octyloxy units enhances self-diffusion within the polymeric matrix, and therefore, during film formation, the cohesion between the polymer chains, and thus, coalescence are promoted [20]. Moreover, polymers which contain side chains that do not strikingly hinder self-diffusion may have a greater cohesive strength than non-branched polymers, based on a firmer anchoring of such macromolecules in the polymeric matrix [20].

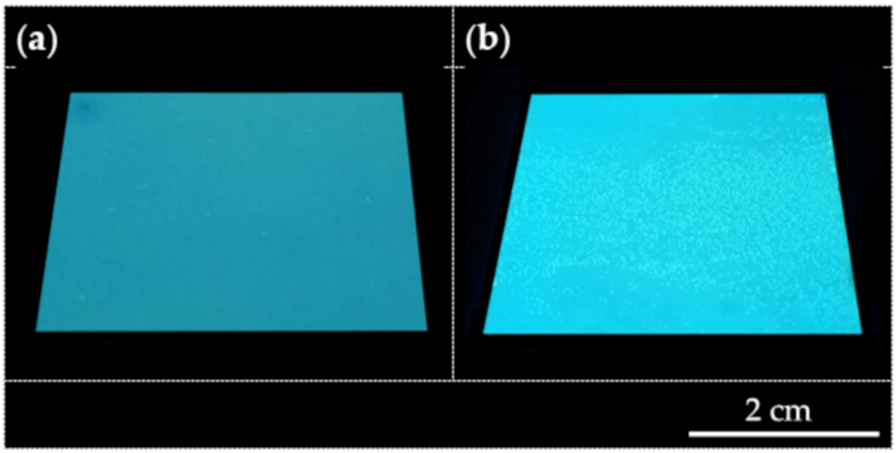

Figure 5. PPM derivatives coatings on polybenzylsiloxane-modified AA2024. (**a**) Surface coated with CO-PPM containing 13.4% of 4-octyloxy side-chains. (**b**) Surface coated with CO-PPM containing 6.1% of 4-octyloxy side-chains.

Remarkably, it is common knowledge that corrosion inhibition may also be favored by the hydrophobic behavior of polymer coatings and the homogeneity of their surface. Advancing and receding contact angles of water on copolymer coatings confirmed the low wettability of the protective films (Table 3). Moreover, the remarkably low contact angle hysteresis (4° and 1°, for 6.1% mol/mol and 13.4% mol/mol octyloxy units) indicates a very smooth and uniform surface (notably, the contact angle hysteresis was even lower than that on AA2024 itself) [1].

Table 3. Contact angles.

Sample	Advancing	Receding
6.1% octyloxy units	104°	100°
13.4% octyloxy units	102°	101°
AA 2024 [(1)]	55°	41°

[1] literature data [1].

3.5. Protective Behavior of PPM-Based Coatings against Corrosion of AA2024

The coatings of the copolymers are an electrical insulating layer deposited on the silane treated surface of aluminum AA2024. Thus, the protective action of the coating against corrosion of the metallic substrate is merely due to a physical barrier effect, aimed to prevent the direct contact between the aggressive environment (i.e., naturally aerated near-neutral 3.5 wt.% NaCl aqueous solution) and the underlying aluminum surface.

Polarization scans are a useful electrochemical method to compare the barrier properties of the here prepared PPM-based coatings containing 6.1% mol/mol and 13.4% mol/mol repeat units with long alkoxy side chains that, extending from the main polymer backbone, act as an internal plasticizer.

Contrary to single-cycle polarization technique (commonly called pitting scan), in which an anodic scan is immediately followed by a backward one, which has been recognized as a valuable tool for the detailed corrosion morphology analysis of aluminum [21–23], anodic polarization provides a faster but more qualitative method to study the corrosion phenomena. In this work, the recorded current density was exploited as a diagnostic parameter to identify the occurrence of localized corrosion.

In the case of the copolymer with 6.1% octyloxy units, excessive porosity (Figure 5b) and/or presence of cracks in the polymer layer resulted into a worst physical barrier effect, in turns detected by a current increase during the polarization test (Figure 6a) due to localized (i.e., pitting) corrosion, thus resulting in aluminum dissolution. This well-known corrosion phenomenon to which Al is susceptible in the presence of chlorides occurs already at OCP for bare aluminum (Figure S3), resulting in a quick increase of the current density to values of many Ma cm^{-2} already at –0.6 V vs. SCE [21–23]. The resulting shift toward more positive potentials for the abrupt increase of the current density for the coated metal (Figure 6a) with respect to the bare one (Figure S3) is due to the barrier-like protective property of the PPM coatings. Therefore, current densities 10^6 times lower (i.e., few Na cm^{-2}) are maintained at potentials even more positive than the OCP and the critical pitting potential of bare AA2024, resulting into a significantly increased resistance towards the aggressive environment.

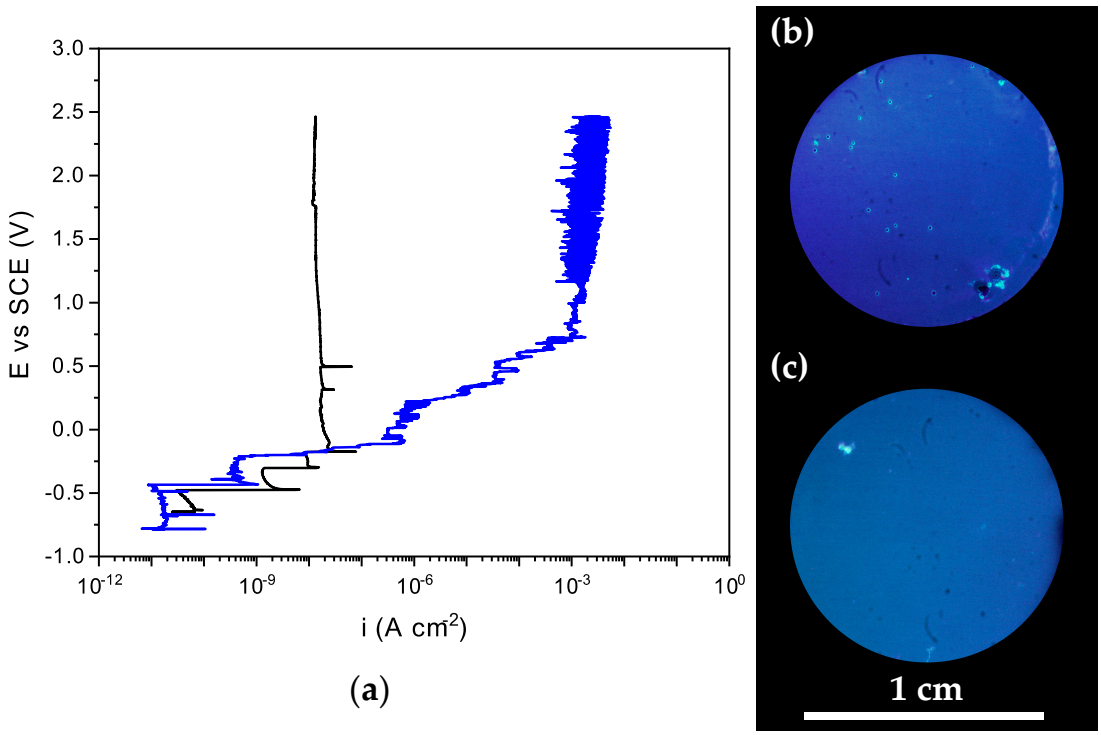

Figure 6. (**a**) Anodic polarization curves for AA2024 coated with copolymer with 6.1% (blue lines) and 13.4% ocytyloxy units (black lines) in naturally aerated near-neutral 0.6 M NaCl solution. Right: Optical microscope pictures (under 395 nm light irradiation) of samples coated with copolmyer containing 6.1% (**b**) and 13.4% octyloxy units (**c**) after polarizations tests.

Best anodic polarization curves recorded for silane treated AA2024 coated with a layer of 6.1% and 13.4% octyloxy units are presented in Figure 6a, where the scans started from OCP (between –0.78 and –0.61 V vs. SCE) as detected after 600 seconds of equilibration between the samples and the solution. For sake of reproducibility, different samples of each copolymer were tested. All data are reported in the Electronic Supporting Information (Figures S4 and S5).

While at the more negative potentials both types of copolymers assure a comparable good protection of the underlying AA2024 (current densities around 10 nA cm^{-2}), the coating prepared with a lower amount of the comonomer exhibited an abrupt increase of the current density starting at ca.

–0.50 V vs. SCE (Figure 6a and Figure S4). This sudden and almost monotonic increase of current (from nA cm^{-2} to mA cm^{-2} within 1 V) is a proof of the limited protection ability of the copolymer with 6.1% octyloxy units, that invariably showed defects after the polarization tests, responsible for the direct metal/solution contact (Figure 6b, and Figures S6 and S7). On the other hand, coatings obtained with the copolymer containing octyloxy units (13.4%) exhibited almost stable current density of 13–30 nA cm^{-2} up to at least 2.5 V vs. SCE (Figure 6a and Figure S5). These results are compatible with very good isolation of the Al surface from the solution by this coating, as a result of an almost complete absence of cracks and holes (Figure 5a, Figure 6c, and Figures S8, and S9) and a low porosity level. To give a clearer quantitative comparison, AA2024 in de-aerated near-neutral 3.5 wt.% NaCl (a less aggressive analog with respect to the aerated solution employed in this study) exhibits passivation current densities around μA cm^{-2} [23], i.e., two orders of magnitude higher than those recorded with the copolymer with 13.4% octyloxy units even applying extremely more oxidizing potentials.

By comparing the performance of the two types of coatings (Figure 6a), it is possible to tentatively attribute the better barrier effect of the copolymer with 13.4% octyloxy units to the higher content of long alkyl side chains that act as a more effective plasticizer by increasing compactness, cohesion, and adhesion ability of the cured films.

As confirmed by DSC (see the previous section), the addition of a comonomer introducing long side chains resulted in a modified PPM with a glass transition temperature (T_g) of 31 °C, lower than pristine PPM of the same molar mass (around 55 °C [1]). Considering that T_g of the copolymers is comparable to the temperatures that an AA2024 manufacture can encounter in real application, additional anodic polarization curves were recorded on aluminum alloy samples coated with the best performing copolymer (13.4% octyloxy groups), by setting the temperature of the 3.5 wt.% NaCl solution at 35 °C, just above the glass transition temperature of the copolymer (Figure S10). The coating, when operating at $T > T_g$, showed, on average, worse corrosion-protective behavior with respect to that at temperatures lower than T_g. The worsening can be attributed to the higher mobility of the polymer matrix that loses, at least partially, its barrier effect by favoring, for example, the permeation of the solution toward the underneath aluminum alloy surface.

Stability of the better performing corrosion-protective coating copolymer (13.4% octyloxy units) was further investigated by applying a constant polarization at 0 V vs. SCE to the aluminum-coated sample for 24 h in naturally aerated near-neutral 0.6 M NaCl solution (Figure 7). Current density, starting from some nA cm^{-2} constantly grew reaching, in three hours, a value around 6 μA cm^{-2} that remained almost stationary for a relatively long period of time (up to 12 h). After some hours characterized by high instability, current density started again increasing progressively up to ca. 100 μA cm^{-2}. The reported trend in the current is coherent with a progressive loss of the barrier effect by the polymeric coating, attributable to both increasing permeation of solution through pores and the formation of defects that grow up in time affecting the integrity of the barrier itself. However, it is apparent that the occurrence of defects is confined to few zones mainly localized close to the borders where some contributions of crevice corrosion can take place (Figure S11). The characteristic "up and down" current spikes are potentially attributable to the initiation of small metastable pits.

The corrosion-protective ability of the best formulated "self-plasticized" polymer coating (i.e., 13.4% octyloxy groups) is in line with the performance already reported for coatings of PPM with addition of siloxanes as an external plasticizer [1], especially in terms of current densities recorded during anodic polarization tests (few nA cm^{-2}). This comparison seems to qualitatively confirm that the design of the self-plasticized PPM approach is a good alternative to the more classical one which is based on the addition of external plasticizers.

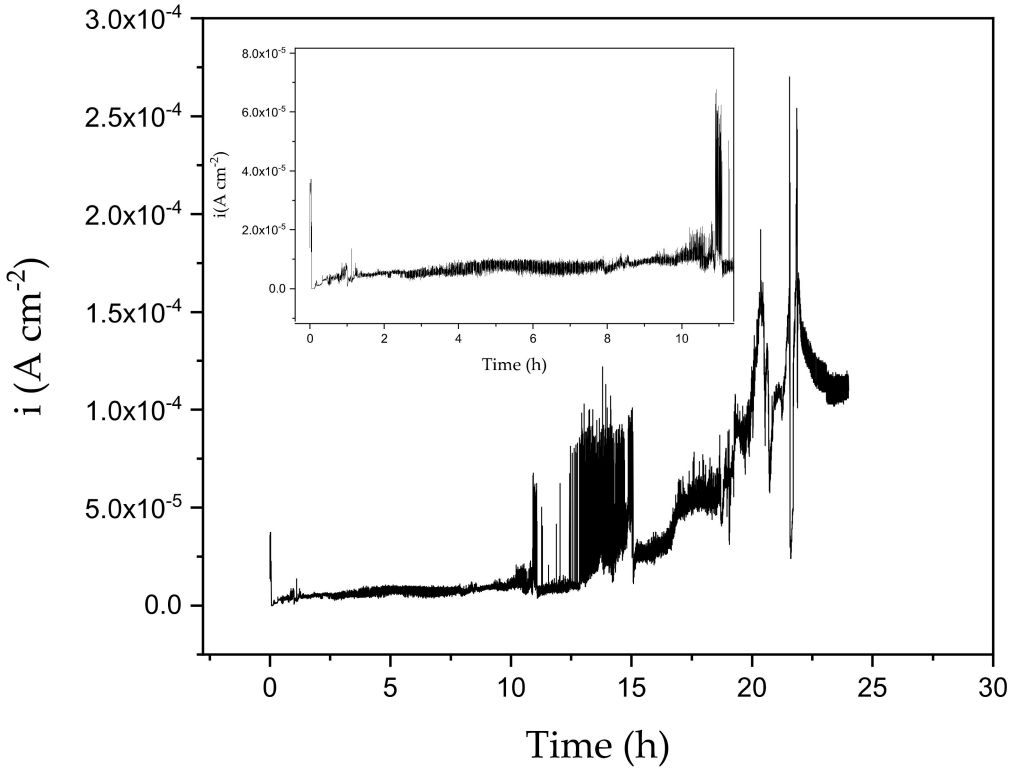

Figure 7. Current density as a function of time for AA2024 coated with a copolymer with 13.4% octyloxy units, polarized at 0 V vs. SCE in naturally aerated near-neutral 0.6 M NaCl solution, duration: 24 h. Inset: Magnification of the first 12 h.

4. Conclusions

Basically, poly(phenylene methylene) (PPM) is a valuable polymer for studies in the area of corrosion prevention coatings due to its thermal stability, hydrophobicity, and fluorescence. The latter facilitates optical detection of inhomogeneities, cracks and other defects caused by pit attacks upon observation under UV-light. However, PPM has to be used with additives, such as plasticizers or polysiloxanes, in order to enable processing into crack-free coating surfaces. Therefore, we aimed at the synthesis of copolymers on the basis of PPM which can be processed to coatings without addition of additives. For this purpose, benzyl chloride and 4-octyloxybenzyl chloride were copolymerized, using tin (IV) chloride as catalyst. Thus, copolymers with 6.1% mol/mol and 13.4% mol/mol octyloxy units were obtained. Notably, fluorescence of PPM was preserved in presence of side-chains on the polymer backbone.

In addition, it was shown that the copolymers are materials with high thermal stability. Further, the alkoxy chains lead to a decrease of the glass transition temperature of the copolymers, confirming the plasticizing effect of the substituent. This finding is line with the viscosity drop at higher fraction of alkyloxy units (13.4% mol/mol).

Gratifyingly, powders of the copolymers can be processed into coatings, providing homogeneous -crack-free surfaces on pretreated AA2024 substrates. The presence of alkoxy side chains along the polymer chains enhances the elasticity and the cohesion of the system, and hence the coating can adapt better to deformation which occurs upon cooling of the coated system prepared by hot pressing.

The isolation of copolymers based on PPM and their corrosion protection ability opens the way for studies on the application of such materials in the area of corrosion protection and monitoring.

Supplementary Materials: The following are available online at http://www.mdpi.com/2076-3417/9/17/3551/s1. Figure S1: SEM image of cross section of AA2024 coated CO-PPM containing 13.4% mol/mol of 4-octyloxy side chains. Figure S2: SEM image of cross section of AA2024 coated CO-PPM containing 6.1% mol/mol of 4-octyloxy side chains. Figure S3: Behavior of uncoated AA2024, in naturally aerated near-neutral 0.6 M NaCl solution.

Figure S4: Reproducibility tests (anodic polarization) for sample AA2024 coated with PPM_6.1%-OcOx. Figure S5: Reproducibility tests (anodic polarization) for sample AA2024 coated with PPM_13.4%-OcOx. Figure S6: SEM image of AA2024 coated CO-PPM containing 6.1% mol/mol of 4-octyloxy side chains. Figure S7: SEM image of cross section of a defect on AA2024 coated CO-PPM containing 6.1% mol/mol of 4-octyloxy side chains after polarization. Figure S8: SEM image of AA2024 coated CO-PPM containing 13.4% mol/mol of 4-octyloxy side chains which shows a uniform and homogenous surface even after polarization (top view). Figure S9: SEM image of cross section of AA2024 coated CO-PPM containing 13.4% mol/mol of 4-octyloxy side chains after polarization. Figure S10: Anodic polarization curves for AA2024 coated with PPM_13.4%-OcOx at 35 °C. Figure S11: optical microscope pictures of PPM_13.4%-OcOx under 24h polarization at 0 V vs. SCE.

Author Contributions: M.F.D. performed the synthesis of the monomers and copolymers. The manufacture of the coatings was performed under supervision of W.C. and M.N.; T.B.S. contributed to the rheology measurements which were performed and designed together with M.F.D.; the corrosion tests were performed by M.M. under supervision of S.P.M.T., and the manuscript was written by M.F.D., W.C. and M.M.

Funding: This research received no external founding.

Acknowledgments: We thank Elena Tervoort for taking SEM images.

Conflicts of Interest: The authors declare no conflict of interest.

References

1. D'Elia, M.F.; Braendle, A.; Schweizer, T.; Ortenzi, M.; Trasatti, S.; Niederberger, M.; Caseri, W. Poly(Phenylene Methylene): A Multifunctional Material for Thermally Stable, Hydrophobic, Fluorescent, Corrosion-Protective Coatings. *Coatings* **2018**, *8*, 274. [CrossRef]
2. Braendle, A.; Schwendimann, P.; Niederberger, M.; Caseri, W. Synthesis and fractionation of poly(phenylene methylene). *J. Polym. Sci. Part A Polym. Chem.* **2018**, *56*, 309–318. [CrossRef]
3. Ellis, B.; White, P. Thermal degradation of polybenzyl. *J. Polym. Sci. Polym. Chem. Ed.* **1973**, *11*, 801–821. [CrossRef]
4. Dreyer, D.; Jarvis, K.; Ferreira, P.; Bielawski, C. Graphite Oxide as a Dehydrative Polymerization Catalyst: A One-Step Synthesis of Carbon-Reinforced Poly(phenylene methylene) Composites. *Macromolecules* **2011**, *44*, 7659–7667. [CrossRef]
5. Hino, M.; Arata, K. Iron oxide as an effective catalyst for the polycondensation of benzyl chloride, the formation of para-substituted polybenzyl. *Chem. Lett.* **1979**, *8*, 1141–1144. [CrossRef]
6. Braendle, A.; Perevedentsev, A.; Cheetham, N.; Stavrinou, P.; Schachner, J.; Mösch-Zanetti, N.; Niederberger, M.; Caseri, W. Homoconjugation in poly(phenylene methylene)s: A case study of non-π-conjugated polymers with unexpected fluorescent properties. *J. Polym. Sci. Part B Polym. Phys.* **2017**, *55*, 707–720. [CrossRef]
7. Muller, P. Glossary of terms used in physical organic chemistry (IUPAC Recommendations 1994). *Pure Appl. Chem.* **1994**, *306*, 1077–1184. [CrossRef]
8. Ferguson, L.; Nnadi, J. Electronic interactions between nonconjugated groups. *J. Chem. Educ.* **1965**, *42*, 529–535. [CrossRef]
9. Rosen, S.L. *Fundamental Principles of Polymeric Materials*; Wiley: New York, NY, USA, 1993.
10. Rahman, M.; Brazel, C.S. The plasticizer market: An assessment of traditional plasticizers and research trends to meet new challenges. *Prog. Polym. Sci.* **2004**, *29*, 1223–1248. [CrossRef]
11. Small, P.A. The diffusion of plasticisers from polyvinyl chloride. *J. Chem. Technol. Biotechnol.* **1947**, *66*, 17–19. [CrossRef]
12. Wypych, G. 13-Plasticizers in various industrial products. In *Handbook of Plasticizers*, 3rd ed.; Elsevier: Toronto, ON, Canada, 2007; pp. 495–605.
13. Immergut, E.H.; Mark, H.F. Principle of Plasticization. In *Plasticization and Plasticizer Processes*; ACS Editorial Library: Washington, DC, USA, 1965; pp. 1–26.
14. Rehberg, C.E.; Fisher, C.H. Properties of Monomeric and Polymeric Alkyl Acrylates and Methacrylates. *Ind. Eng. Chem.* **1948**, *40*, 1429–1433. [CrossRef]
15. Tavares, A.; Schneider, P.H.; Merlo, A.A. 3,5-Disubstituted Isoxazolines as Potential Molecular Kits for Liquid-Crystalline Materials. *Eur. J. Org. Chem.* **2009**, *2009*, 889–897. [CrossRef]

16. Spreti, N.; Brinchi, L.; Germani, R.; Mancini, M.V.; Savelli, G. A New Carrier for Selective Removal of Heavy Metal Ions from Aqueous Solutions through Bulk Liquid Membranes. *Eur. J. Org. Chem.* **2004**, *2004*, 3865–3871. [CrossRef]
17. Zhao, Y. Nanoparticles and Nanoparticles Compositions. U.S. Patent 2013/0101516 A1, 25 April 2013.
18. Gunes, D.; Yagci, Y.; Bicak, N. Synthesis of Soluble Poly(p-phenylene methylene) from Tribenzylborate by Acid-Catalyzed Polymerization. *Macromolecules* **2010**, *43*, 7993–7997. [CrossRef]
19. M'Hiri, T.; Catusse, C.; Catusse, R.; Dubry, J.L.J. Polymerization of benzyl alcohol and its derived compounds with an ion exchange resin. *React. Kinet. Catal. Lett.* **1983**, *22*, 425–428. [CrossRef]
20. Banker, G.S. Film Coating Theory and Practice. *J. Pharm. Sci.* **1966**, *55*, 81–89. [CrossRef] [PubMed]
21. Trueba, M.; Trasatti, S.P. Electrochemical approach to repassivation kinetics of Al alloys: Gaining insight into environmentally assisted cracking. *Corros. Rev.* **2015**, *33*, 373–393. [CrossRef]
22. Comotti, I.M.; Trueba, M.; Trasatti, S.P. The pit transition potential in the repassivation of aluminium alloys. *Surf. Interface Anal.* **2013**, *45*, 1575–1584. [CrossRef]
23. Truba, M.; Trasatti, S.P. Study of Al alloy corrosion in neutral NaCl by the pitting scan technique. *Mater. Chem. Phys.* **2010**, *121*, 523–533. [CrossRef]